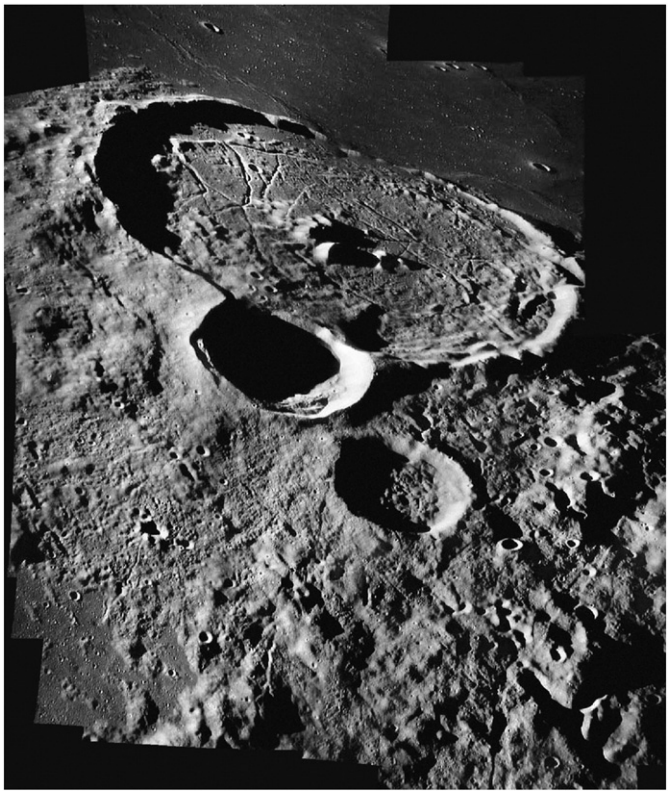

Fig. 2. Oblique view from the north of the lunar floor-fractured crater Gassendi, 110 km in diameter. Note the shallow floor, the multiple floor fractures, and the lavas that flooded the southern part of the crater from Mare Humorum to the south. The central peaks rise higher than portions of the rim crest. Mosaic of Apollo 16 images AS16-120-19278 through AS16-120-19313.

(compare Figs. 3B and 5A). The western dome-like feature is irregularly shaped, about 12 km by 17 km, and contains a network of fractures each less than about 1 km in width on its summit and southern part. The eastern dome-like feature is also irregularly shaped, about 9 km by 15 km, and contains less well-developed fractures on its southeastern flank. In lunar floor-fractured craters, as exemplified by the larger crater Gassendi (Fig. 2), the uplift of the entire flat crater floor (and central peak), the creation of a moat outward of the uplifted central floor (Fig. 4A), and the flooding of the moat are the evidence that supports the interpretation of a shallow intrusion and inflation of a broad sill-like structure. For the crater on Mercury (Fig. 3B, C), however, in addition to more moderate floor uplift than for Gassendi, floor modification appears more localized and focused at these two dome-like locations.

This floor-fractured crater appears to be most similar to lunar Class IVB of Schultz (1976), as exemplified by the lunar crater Gaudibert, at 33-km diameter a crater comparable in size to the crater on Mercury, located along the northeastern edge of Mare Nectaris (10.9°S, 37.8°E) (Fig. 4). Class IV lunar floor-fractured craters are shallow and characterized by a narrow floor moat (usually v-shaped in cross-sectional profile) adjacent to the inner wall. The interior border of the moat is often ridge-like, and in Gaudibert (Fig. 4) the border is in places at a higher elevation than the rim (Schultz, 1976) (compare Figs. 3B and 4A). Schultz (1976) interpreted the differences between Class III (e.g., Gasssendi, Fig. 2) and Class IV (e.g., Gaudibert, Fig. 4) lunar floor-fractured craters to be to the result of differences in the size of the initial crater and its corresponding morphology (greater development of wall terraces and greater expanse of flat floor in larger craters; Pike, 1980), and he introduced cross-sectional interpretations of sill emplacement and floor fracturing that were similar in process but differed in detail (compare his Figs. 10 and 15).

Gaudibert also shows interior dome-like features, and there are hints of the presence of associated fractures (Fig. 4A). Furthermore, Gaudibert occurs along the margin of Mare Nectaris, and Clementine images (Fig. 4) show the proximity of the low-albedo mare deposits and the occurrence of low-albedo material on the southern floor of the Gaudibert crater, in association with a rimless depression of possible volcanic origin. The Mercury example (Fig. 3A) occurs along the margin of smooth plains interpreted to be of volcanic origin (Head et al., 2008, 2009-this issue). On the basis of these associations and characteristics, we interpret the features in the Mercury crater to be the result of local sill-like intrusions, following the general interpretations of Schultz (1976) for lunar craters, but in the Mercury case (and perhaps in Gaudibert) we interpret the sills to have a more laccolith-like structure, where the central part of the sill inflates, upbowing and fracturing the overlying substrate (Figs. 3B, C and 4A). Rimless depressions on crater floors on Mercury, detected in MESSENGER images, have also been interpreted as evidence of near-surface magmatic activity (Gillis-Davis et al., 2009-this issue), although they are not associated with extensive floor-fracturing.

The global distribution of floor-fractured craters on Mercury is currently unknown. As pointed out by Schultz (1977), the illumination geometry is critical to detection of floor-fractured craters, with shallow crater topography and detailed tectonic structure much more obvious at low Sun elevation angles than at high. The detection

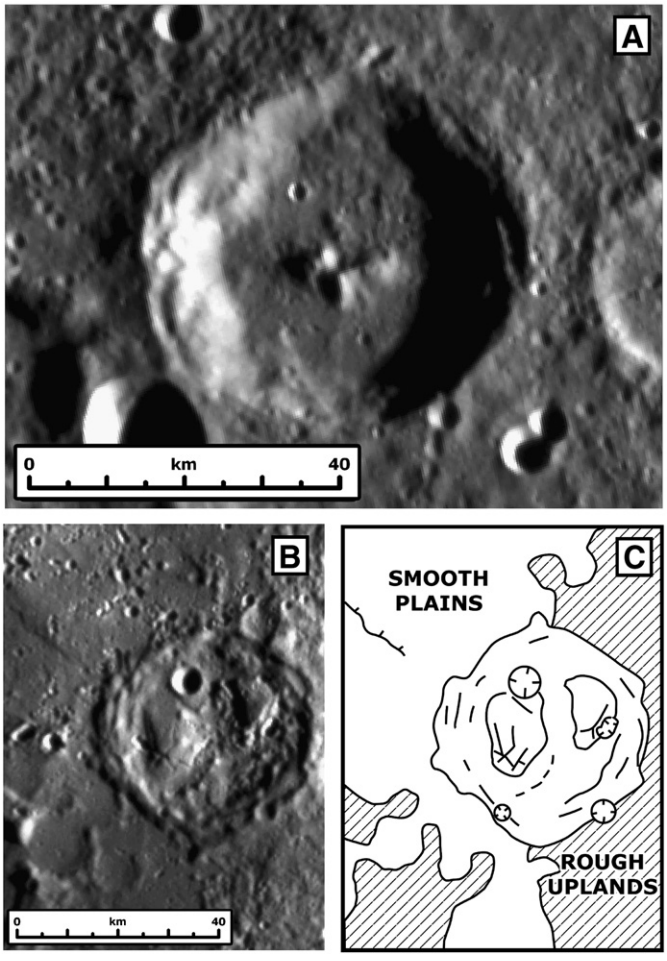

Fig. 3. Relatively fresh crater on Mercury compared with a floor-fractured crater observed during the first MESSENGER flyby. (A) Typical relatively fresh impact crater about 49 km in diameter on Mercury (24.3°N, 105.4°E). MDIS narrow-angle camera (NAC) image EN0108826782M. (B) Floor-fractured ~35-km-diameter crater on Mercury (7.5°N, 104.3°E) (see Head et al., 2008). MDIS NAC image EN0108826977M. (C) Sketch map of major features in (B) showing domes and fractures and proximity to smooth plains.